



ارائه شده توسط:

سایت ترجمه فا

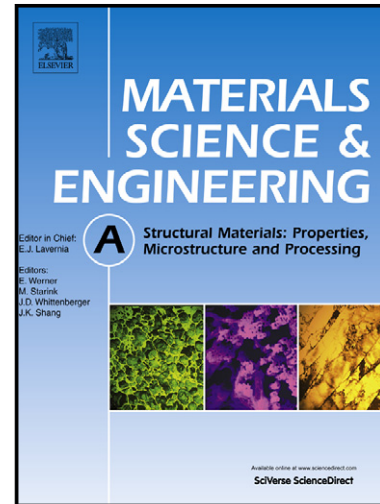
مرجع جدیدترین مقالات ترجمه شده

از نشریات معتبر

Author's Accepted Manuscript

A new severe plastic deformation technique
based on pure shear

A.R. Eivani



www.elsevier.com/locate/msea

PII: S0921-5093(14)01524-X
DOI: <http://dx.doi.org/10.1016/j.msea.2014.12.024>
Reference: MSA31841

To appear in: *Materials Science & Engineering A*

Received date: 3 September 2014
Revised date: 5 December 2014
Accepted date: 8 December 2014

Cite this article as: A.R. Eivani, A new severe plastic deformation technique based on pure shear, *Materials Science & Engineering A*, <http://dx.doi.org/10.1016/j.msea.2014.12.024>

This is a PDF file of an unedited manuscript that has been accepted for publication. As a service to our customers we are providing this early version of the manuscript. The manuscript will undergo copyediting, typesetting, and review of the resulting galley proof before it is published in its final citable form. Please note that during the production process errors may be discovered which could affect the content, and all legal disclaimers that apply to the journal pertain.

A new severe plastic deformation technique based on pure shear

A. R. Eivani*

School of Metallurgy and Materials Engineering, Iran University of Science and Technology (IUST), Tehran, Iran.

Abstract

Pure shear extrusion (PSE) is introduced as a new severe plastic deformation (SPD) technique. The new SPD process provides the possibility of severely deform metals and alloys in a combined mode of pure and simple shear with the opportunity of changing the ratio of pure to simple shear. The process is fundamentally based on what in the literature known as pure shear, in which, a square deforms to a rhombic alongside its diagonals. The deformation zone in PSE process is composed of two sections, i.e., upper and lower deformation zones. In the upper deformation zone, an initial square cross section of a sample gradually changes shape to a rhombic while keeping a constant cross sectional area. The constancy of the cross sectional area certifies no velocity change and therefore, no strain in the direction perpendicular to the cross section of the sample leading to a plane-strain deformation. In the lower deformation zone, the

*Corresponding author; Email: aeivani@iust.ac.ir , Tel: +98 (0) 21 77 240 540, Fax: +98 (0) 21 77 240 480.

sample gradually gains its initial geometry back by an inverse deformation regarding the upper zone. The constancy of cross section of the sample provides the possibility of repeating the deformation process which makes the PSE as a new candidate for SPD processing of metals and alloys. Effective strain is estimated using a geometrical approach. AA1050 aluminum alloy is deformed up to two passes using PSE in order to verify the feasibility of SPD processing by PSE.

Keywords: Severe plastic deformation; Bulk nanostructured alloys; Pure shear extrusion.

1 Introduction

In recent years, nanostructured metals and alloys have gained significant interest in academic research due to their unique physical and mechanical properties [1-5]. Among every production technique of bulk nanostructured materials (BNM), severe plastic deformation has shown remarkable capacities for in different metals and alloys [6-9]. SPD techniques, e.g., equal channel angular extrusion (ECAE) [10-12], high pressure torsion (HPT) [12-14], twist extrusion (TE) [15] accumulative roll bonding (ARB) [16], repetitive corrugation and straightening (RCS) [17], multi-directional forging (MDF)

[18], cyclic expansion extrusion (CEE) [19] and recently developed simple shear extrusion (SSE) [20, 21] have been developed towards producing BNM [22] in different metals and alloys [6-9]. Despite of having different technological characteristics, these processes are normally used for similar purposes to produce BNM, however, the deformation modes rang from pure shear to simple shear and as well, from monotonic loading to cyclic and cross loading. It has been shown by Segal [23] that the deformation state, i.e., simple or pure shear, causes significant differences in the response of the material towards grain refinement. It is found [23] that application of simple shear provides a short stage of continuous evolution, early localization and cross loading resulting in a considerable grain refinement while pure shear may not play a similar role. However, it should be mentioned that the process which was used for applying pure shear in that study [23] was rolling which obviously does not provide the capacity of keeping the cross section of the material constant. Therefore, it is not surprising if a long stage of continuous evolution, planar high angle grain boundaries and monotonic loading with effective reduction of material cross section are among the findings. One may add that rolling is associated with redundant work which results in an

inhomogeneous deformation in addition to not maintaining a constant cross section and therefore, may not be a most suitable process for SPD.

The lack of the presence of a SPD process providing the possibility of applying homogeneous pure shear deformation and returning the initial shape of the sample has made it quite difficult for investigating the effect of deformation mode, i.e., simple and pure shear, on microstructural evolution. The deformation mode in most of the well-known SPD processes, e.g., ECAE, HPT, TE and SSE, is simple shear or most significantly governed by simple shear [23]. The rest of SPD processes, e.g., ARB, RCS, MDF and CEE which act totally or partly in pure shear, are based on traditional metal forming processes such as rolling, extrusion and forging [16-19]. These processes are inherently involved with redundant work [24] which causes an inhomogeneous deformation and consequently a nonhomogeneous microstructure and mechanical properties throughout the processed sample. To the knowledge of the author, no SPD technique exists for applying strain in non-simple shear or in pure shear deformation state without redundant work.

Recently, pure shear extrusion (PSE) is introduced as a new SPD technique [25]. In this article, the process is thoroughly investigated. The process defines the possibility of applying combined deformation state of pure and simple shear without redundant work and strain inhomogeneity. It is claimed that PSE is a single SPD process by which it is possible to apply a homogeneous combined pure and simple shear deformation on materials. The process introduced in this study provides the possibility of a fair comparison between the efficiency in grain refinement by applying simple and pure shear which may be the subject of study in future research activities. The possibility of severe deformation of materials with different ratios of pure and simple shear may result in unique applications for this process.

2 Theory

2.1 Purer shear extrusion

The principles of pure and simple shear are schematically shown in Fig. 1 [24]. If an element is subjected to state of shear strain, Fig. 1 (a), the distortion causes equal angular changes as shown in Fig. 1 (b). The shear strain associated with near faces is $\gamma/2$ as illustrated in Fig. 1 (b) which describes pure shear strain condition. Fig. 1 (c)

describes the simple shear deformation mode in which the shear strain is equal to γ

[24].

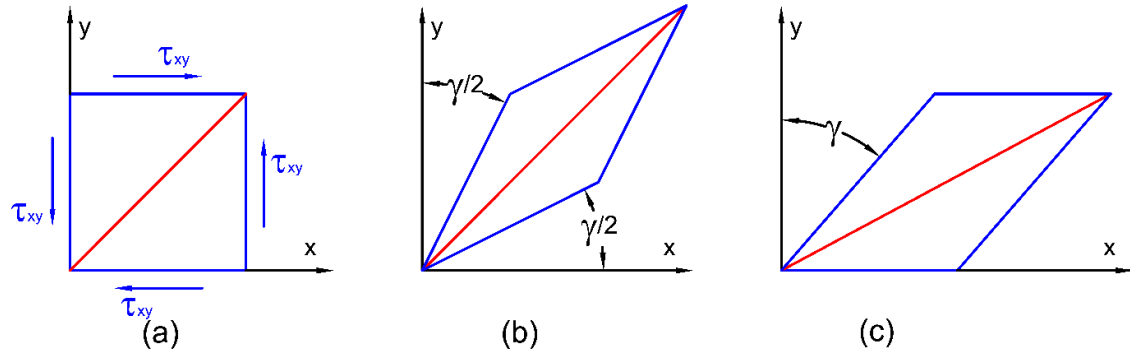


Figure 1- Shear strain states, (a) imposing shear stress, (b) pure shear and (c) simple shear condition.

The principles of PSE, based on the pure shear explained in Fig. 1 (b), are schematically shown in Fig. 2, where two sections of upper (zone II) and lower (zone III) deformation zones are joined at a conjunction plane, denoted by $P - P'$ in the figure. The sample has to be inserted in the entry channel (zone I) and pressed using a ram. The PSEed sample will have to leave the die from the exit channel (Zone IV). It is as well possible to conjunct the two upper and lower deformation zones using a prismatic region with a constant cross section as plane $P-P'$ at which no deformation occurs. This part would be an optional section of PSE die. However, due to the friction between the walls of the relaxation zone and the surfaces of the deforming sample, the existence of this part would definitely help the deforming sample to fill in the die channel more completely. In

addition, by introducing a relaxation zone, the sharp corners of the conjunction plane are deleted and stress concentration and the chance of die breakage reduces.

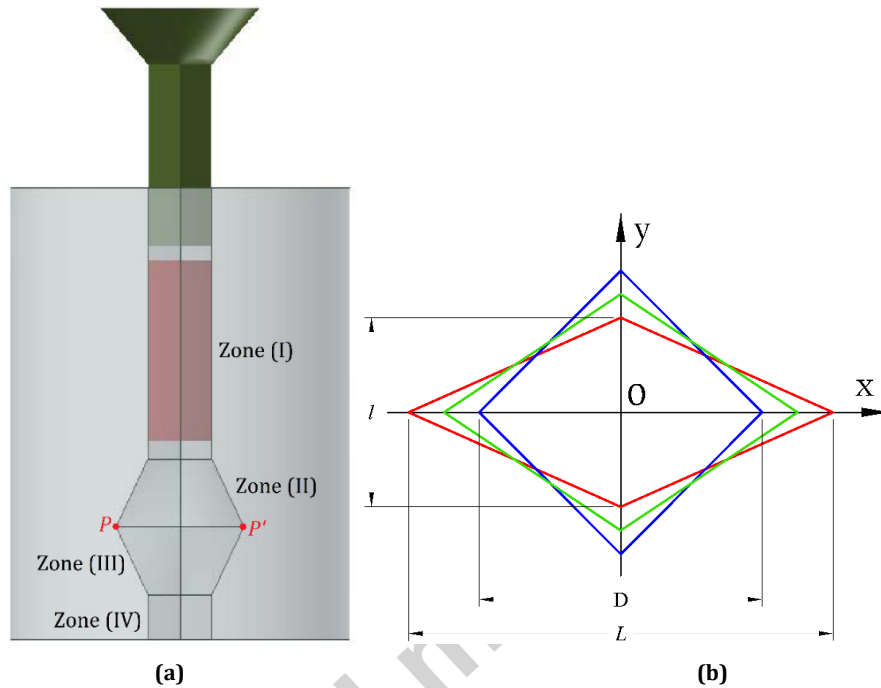


Figure 2- (a) Schematic illustration of pure shear extrusion, showing the ram in green color, the sample in red in zone I (the entry channel), the upper (zone III) and lower (zone IV) deformation zones and the exit channel (zone V) and (b) Top view of PSE deformation illustrating the changes of the cross section of the sample at the half course of PSE deformation.

In the upper deformation zone, the square cross section of a sample gradually changes into a rhombic while keeping a constant cross sectional area at every instant of deformation. The constancy of the cross sectional area certifies no velocity change and therefore, no strain in the direction perpendicular to the cross section of the sample and a plane-strain deformation. In the lower deformation zone, the sample gains its initial shape back in a reverse deformation cycle with regard to the upper zone. No permanent change in the geometry of the deformed sample provides the possibility of repeating the

process for more than one pass and therefore, may stand as a new technique for SPDing of metals and alloys.

The top view of PSE deformation from the upper surface to the conjunction plane of the upper and lower deformation zones is shown in Fig. 2 (b). The changes of the cross section of the sample at the half course of PSE deformation, i.e., a square to a rhombic, can be seen in this figure. At the onset of deformation, an initial square cross section changes to rhombic with small ratio of long to short diagonals. By continuation of deformation, the ratio of the large to short diagonals of the rhombic increases and reaches a maximum at the conjunction plane.

As it was stated above, there is no variation in cross sectional area of the sample in PSE process. In order to this condition be respected, one may write

$$W^2 = \frac{1}{2}(L * l) = \frac{1}{2}D^2 \quad \text{Equation 1}$$

where W and D are the side and diagonal of the initial square cross section and L and l are the long and short axes of the rhombic, respectively (as shown in Fig. 2 (b)).

Therefore,

$$l = 2 \frac{W^2}{L} = \frac{D^2}{L} \quad \text{Equation 2}$$

2.2 Calculation of strain in PSE

In order to estimate the equivalent strain in one PSE pass of deformation, all 9 components of strain should be calculated. Since there is no change in the cross sectional area of the sample, it may be assumed that the velocity of deforming material is constant through the height of the deformation zone perpendicular to the cross section of the sample. Therefore, there is no deformation perpendicular to the $X - Y$ plane, i.e., the deformation is plane strain, and $\varepsilon_{zz} = \gamma_{xz} = \gamma_{yz} = 0$. The rest of nonzero strain components may be calculated as follows.

2.2.1 Deformation of a rectangular element in PSE

In order to evaluate the strain in PSE process, a geometrical approach is used. This approach has been previously used for calculation of strain in other SPD processes, e.g., ECAE [26-28]. For strain calculation, deformation of a small two-dimensional element, $ABCD$, is considered as illustrated in Fig. 3. All four sides of the square make an angle of $\pi/4$ with x -axis. After half way deformation by PSE during which the square moves towards the conjunction plane of the upper and lower deformation zones ($P - P'$ in Fig.

2 (a)), the angles between the sides of the square and x -axis are changed to α and the square $ABCD$ to rhombic, $A'B'C'D'$, shown in Fig. 3 (c). Rhombic $EFGH$ in Fig. 3 (b) shows the intermediate shape of the element $ABCD$ during deformation when each side of the rhombic makes an angle θ with x -axis. In order to facilitate the calculation of strain components in x and y directions, the origin of coordinate system is set at point O and the axes of rectangular coordinate system are placed on the diagonals of the square and the rhombic.

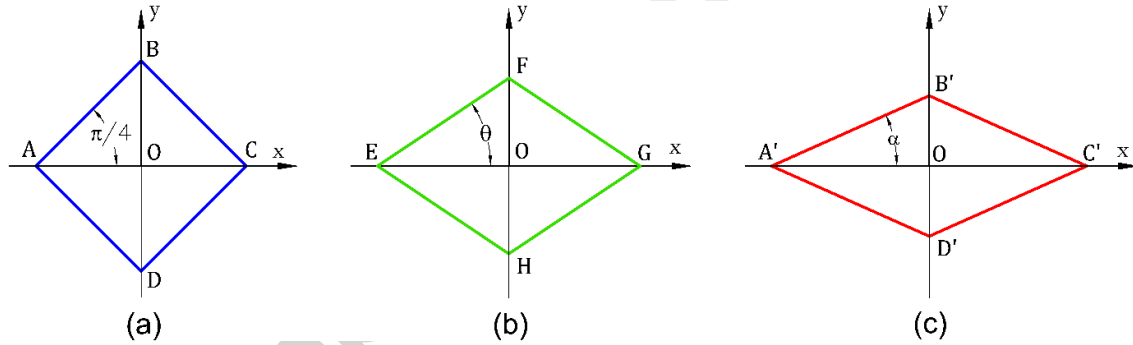


Figure 3- Changes in the geometry of a small two-dimensional element (a) before PSE, square $ABCD$, (b) during the process, rhombic $EFGH$ and (c) after PSE, rhombic $A'B'C'D'$.

By considering the shape change from square to rhombic, it can be seen that lines AB , BC , CD and DA respectively change to $A'B'$, $B'C'$, $C'D'$ and $D'A'$ by PSE deformation. Due to symmetry, the changes of the four lines are exactly similar,

therefore, line AB is chosen for calculations of strain components. It is clear that by changing line AB to $A'B'$, the length of the line with respect to x - and y -axes changes which indicates that normal strains in x - y plane are active. In addition, the angle between AB and the x -axis changes from $\pi/4$ to α between $A'B'$ and the x -axis. This indicates the existence of shear strains.

Normal strain component in x and y directions

The components of strain in x and y directions may be calculated by comparing the changes in the length of the line AB in x and y directions before and after deformation. Dimensions of the line AB in x and y directions are equal with OA and OB , respectively. After deformation, the length of the lines OA and OB changes to OA' and OB' , respectively. Therefore, the strain component in x direction may be computed as

$$\varepsilon_x = \ln \left(\frac{\overline{OC'}}{\overline{OC}} \right) = \ln R \quad \text{Equation 3}$$

Similarly, the strain component in the y direction

$$\varepsilon_y = \ln\left(\frac{\overline{OB'}}{\overline{OB}}\right) = \ln\left(\frac{\overline{OC}^2}{\overline{OC}\overline{OC'}}\right) = \ln\left(\frac{\overline{OC}}{\overline{OC'}}\right) = -\ln R \quad \text{Equation 4}$$

One should note that for calculations in Eq. (4), the equality $\overline{OB} = \overline{OC}$ is used and the conditions of Eq. (2) are reproduced in which one may write $\overline{OB'} = \frac{\overline{OC}^2}{\overline{OC'}}$. In addition, as mentioned before, the strain component in z direction is zero, $\varepsilon_z = 0$. It is clear that $\varepsilon_x + \varepsilon_y + \varepsilon_z = 0$ which is expected according to the incompressibility conditions of metals during plastic deformation.

Shear strain components in PSE (γ_{xy})

For calculation of the shear strain components, the variations in the angles between the line AB with respect to the x and y axes are considered. The angle is $\pi/4$ before PSE and changes to α after the process.

$$\gamma_{xy} = \tan\left(\frac{\pi}{4} - \alpha\right) = \sec 2\alpha - \tan 2\alpha \quad \text{Equation 5}$$

Since

$$\alpha = \tan^{-1} \frac{l}{L} = \tan^{-1} \frac{D^2}{L^2} \quad \text{Equation 6}$$

therefore,

$$\gamma_{xy} = \frac{\left(\frac{L}{D}\right)^2 - 1^2}{\left(\frac{L}{D}\right)^2 + 1^2} = \frac{R^2 - 1}{R^2 + 1} \quad \text{Equation 7}$$

Since, there are two components for shear strains:

$$\gamma_{xy} = 2 \left(\frac{R^2 - 1}{R^2 + 1} \right) \quad \text{Equation 8}$$

Details of the calculations of shear strain components are presented in Appendix A.

2.2.2 Equivalent strain

The most general expression for calculating equivalent strain is

$$\varepsilon_{eq} = \sqrt{\frac{2}{9} \left[(\varepsilon_x - \varepsilon_y)^2 + (\varepsilon_x - \varepsilon_z)^2 + (\varepsilon_y - \varepsilon_z)^2 \right] + \frac{1}{3} (\gamma_{xy}^2 + \gamma_{xz}^2 + \gamma_{yz}^2)} \quad \text{Equation 9}$$

By replacing the strain components in Eqs. (3), (4) and (8) into Eq. (9), one may obtain

$$\varepsilon_{eq} = \frac{2}{\sqrt{3}} \sqrt{(\ln R)^2 + \left(\frac{R^2 - 1}{R^2 + 1} \right)^2} \quad \text{Equation 10}$$

If the deformation is repeated for N passes, the total strain, ϵ_{tot} , can be calculated as in

Eq. (11)

$$\epsilon_{tot} = \frac{2N}{\sqrt{3}} \sqrt{(\ln R)^2 + \left(\frac{R^2 - 1}{R^2 + 1}\right)^2} \quad \text{Equation 11}$$

3 Experimental procedure

Half of the PSE die used in this investigation is shown in Fig. 4. The entry channel was a 20 mm side square cross section and 120 mm in length. The deformation zone was composed of two sections of 25 mm height. A 10 mm long relaxation zone was considered as clear between the two upper and lower deformation zones. The height of the exit channel was 20 mm. A split die was used to avoid stress concentration at the corners and to facilitate easy removal of the specimens. Extrusions were conducted using a hydraulic press of 400 t capacity. AA1050 aluminum alloy with the chemical composition shown in Table 1 was used in order to verify the application of PSE for SPD processing. Rectangular samples of 19.8×19.8×100.0 mm were machined from extruded rods. In order to dispose the effects of previous deformation on the results, the samples were fully annealed at 350 °C for 1 hr.

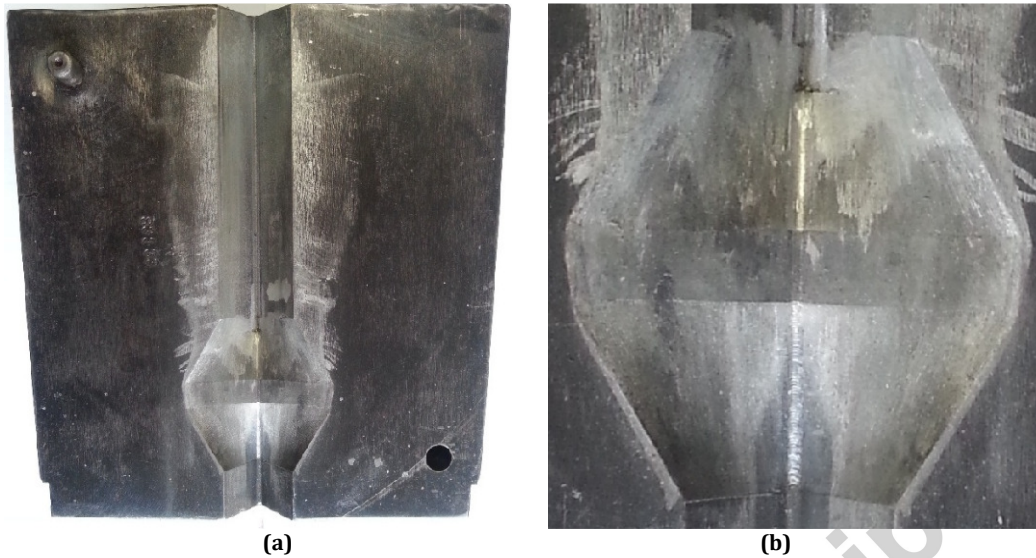


Figure 4- (a) Half of the pure shear extrusion die, (b) close-up view of the deformation zone.

Optical microscopy with polarized light was used to investigate the initial microstructures of the samples as well as the efficiency of the annealing treatment in relieving effects of the previous deformation. The nanostructures of the PSEed samples were investigated using electron backscatter diffraction (EBSD). Samples were prepared through the conventional procedure, starting from mechanical grinding and ending with electrolytic polishing (17 V; 80 s; flow rate: 15; electrolyte: 7.8% perchloric acid, 9% water, 73.1% ethanol and 10% butylcellulose; temperature: 0 °C). EBSD was performed using a JEOL 6500 scanning electron microscope (accelerating voltage: 25 kV; tilt angle: 70 °; working distance: 25 mm; step sizes: 0.5 μm). Orientation contrast data were analyzed with the HKL analyzing software. Subgrains were detected by setting a critical value of 15° as the minimum misorientation value of high angle grain

boundaries (HAGBs). The minimum misorientation value of low angle grain boundaries (LAGBs) was set to be 1 °.

Brinell hardness measurements were taken on normal plane to extrusion direction in order to investigate the homogeneity of strain distribution on the work-piece. Brinell hardness were determined with a ball of 2.5 mm diameter and a test force of 15.625 kg.f applied for 40 s.

4 Results and discussion

Variations of strain components and equivalent strain by R

The variations of ϵ_x and ϵ_{xy} as well as ϵ_{eq} with diagonal ratio, R , are illustrated in Fig. 5.

It is clear that by increasing R , the shear component of strain increases till it attains a constant value approximately at $R=5$. The normal component of strain and the equivalent value consistently increase by increasing R .

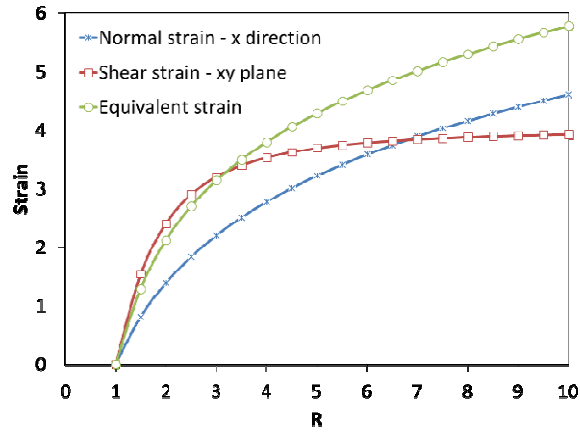


Figure 5- Variations of strain components and equivalent strain with R.

In order to understand the reason behind the fact that the shear strain attains a constant value approximately at $R=5$, the geometries of the initial square with no deformation, the rhombic after half-way deformation by PSE with R equal to 1.5, 2, 3, 5 and 10 are illustrated in Fig. 6. It is clear that when R is larger than a critical value, e.g., 5, further increase in R negligibly change the angle α . Therefore, shear strain does not vary considerably by increasing R beyond 5. It is clear that the change in the length of the diagonal of the rhombic which determines the normal strains continuously increases with R and so does the normal strain components.

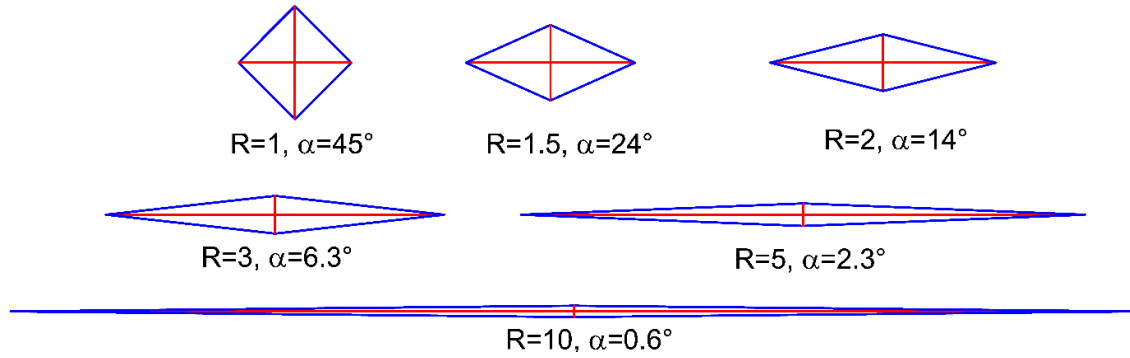


Figure 6- Cross section of the sample at the conjunction plane of PSE dies with at different values for R .

4.1 Simple shear by PSE

Since most of the SPD processes apply simple shear, it is interesting to verify if it is possible to apply deformation in simple shear mode using PSE. In order to apply simple shear deformation on a sample, the values of normal strain components must be equal to zero. By equating either of normal strain components in Eqs. (3) or (4), one may notice that only at $R = 1$, it is possible to obtain zero normal strain which indicates no deformation. In such a case, the shear strain would be zero as well. Therefore, there is no possibility to apply only simple shear using PSE.

In Fig. 7, the ratio of normal to shear strains is presented as a function of R . It should be noted that for calculation of the ratio, equivalent strains are calculated, once only with considering the normal strains and once only with shear strains. It is clear that the share of simple and pure shear deformations vary by changing the diagonal ratio of the PSE

process which provides a broad range of strain states for SPD processing of metals and alloys. The fact that the ratio is always greater than 1 indicates that the governing deformation mode in PSE is pure shear.

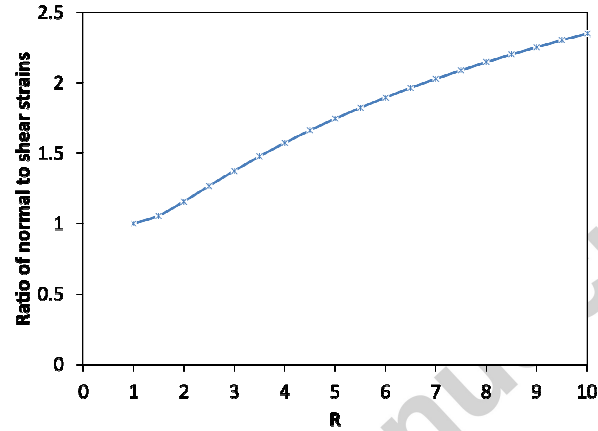


Figure 7- Ratio of normal to shear strains at various R .

Optimum R value

SPD processes are designed to apply heavy strains on the materials. As shown in Fig. 5, the equivalent strain increases as R increases and therefore, for acquiring very large strain in the material, one may be suggested to use a die with large R . The SPD processes including PSE as well are designed to repeat the deformation with no significant change in the geometry of the sample [22]. Therefore, another method to apply high strains is to repeat the process for a large number of passes. However, as it is shown in Fig. 6, with increasing R to values larger than 3, very narrow deformation

zone at the sharp corners forms which makes it quite difficult for the deforming material to move against the die walls. The thinning of the deformation zone may not worth the increase in strain in one pass. Therefore, in order to predict a relatively optimum value for R , the imposed strain is normalized over the frictional surface and presented in Fig. 8. The method used for calculation of the frictional surface, assuming that the deforming sample is in full contact with the die walls is presented in Appendix B.

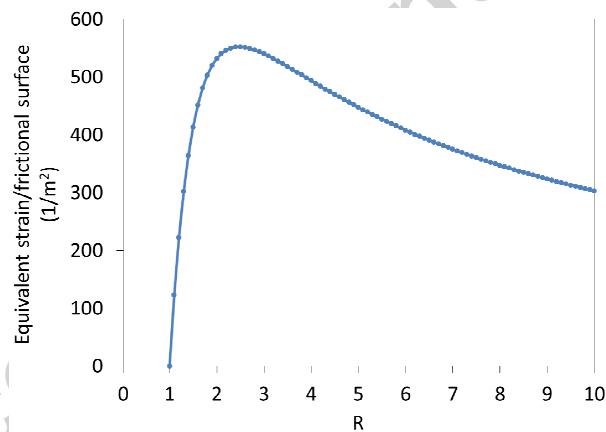


Figure 8- The ratio of equivalent strain over frictional surface as a function of R .

It is clear from Fig. 8 that the normalized strain over frictional surface increases initially up to a value of 2.45 for R . In fact, it may be roughly concluded that up to this point, the increase in R which leads to a higher value for strain worth the addition of frictional

surfaces. However, beyond 2.45 for R , the normalized value reduces, indicating that a higher fraction of energy spent in PSE process is consumed to overcome the friction.

4.2 Feasibility study of SPD by PSE

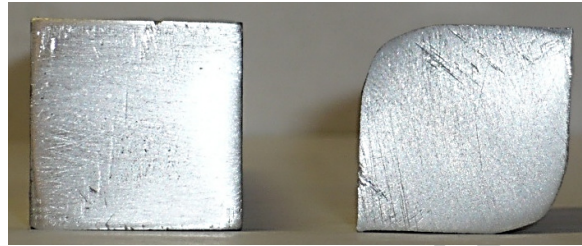
4.2.1 Geometrical considerations

A sample of AA1050 aluminum alloy in the deformation zone is illustrated in Fig. 9 (a).

It is clear that the sample almost totally fills in the deformation zone. This may be considered as an indication for homogeneous deformation throughout the sample. It is clear that a prismatic non-changed cross section (relaxation zone) is observed at the conjunction between the upper and lower deformation zone. It should be considered that no deformation occurs at the relaxation zone. The deformation zone may only help the sample to fill more completely in the deformation zone and to remove the stress concentration at the sharp corners of the conjunction between the upper and lower deformation zones.



(a)



(b)

Figure 9- (a) An AA1050 specimen in the midway of deformation by PSE and (b) Cross section of the sample before (left) and after (right) PSE. It can be seen that the materials almost totally fills in the exit channel of the die.

The cross section of the sample, before and after PSE is illustrated in Fig. 9 (b). One may note that the sample gains back its initial shape which confirms the ability of PSE to be used as a SPD process. Two curved corners up-left and down-right in the deformed sample (the right sample in Fig. 9 (b)) are observed indicating underfilling. In exception of these two regions, the sample almost fully fills in the exit die channel after a pass of PSE which indicates a relatively homogeneous deformation has occurred.

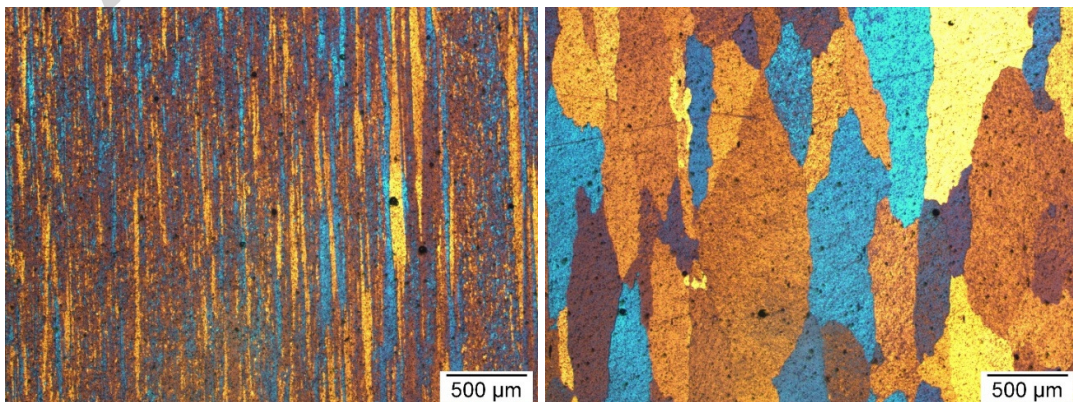
Although there are two curved corners indicating underfilling in the deformed sample, however, it should be noted that the samples are deformed with $R = 2$, in which a strain of 2.12 is imposed (Eq. (10)). If the same strain is to be imposed by the most widely SPD process used, e.g., ECAE, it needs to be done in two passes of deformation using a die of 90° angle or in one pass using a die with an acute angle of 57° [29, 30]. ECAE deformation using a die with an acute angle requires very high pressure [31, 32] in addition to the fact that the die must provide enough strength and the deforming material enough workability to not failure during deformation. Assuming that manufacturing such die is possible and metallic samples can resist the heavy deformation in one pass without failure and the press and the die can afford such high required pressure, the occurrence of a large dead metal zone or underfilling is inevitable [33].

Alternatively, if one may suggest to use a 90° ECAE die and apply the strain in two passes which seems to help overcome or at least reduce the underfilling and dead zone formation problems, a similar suggestion may stand valid for PSE to use a die with $R=1.365$ and deform the sample for two passes. By using a die with small R , e.g., 1.365,

the underfilling would definitely shrink. Therefore, the underfilling observed in the PSEd sample at strain of 2.12 may not be a serious disadvantage of the process. This issue needs to be clarified in further investigations.

4.2.2 Microstructural evolution

The initial microstructure of the sample in as-rolled and as-annealed conditions are shown in Fig. 10. It is clear that the microstructure of the as-rolled sample is composed of elongated grains formed during rolling. In order to dispose the effects of previous deformation steps on the final results of this investigation, the samples were fully annealed before PSE. The microstructure of the sample after annealing at 350 °C for 1 hr is shown in Fig. 10 (b). It can be clearly seen that the deformed and elongated microstructure is totally annihilated and a coarse microstructure with an average grain size of $600\pm 50\ \mu\text{m}$ has formed.



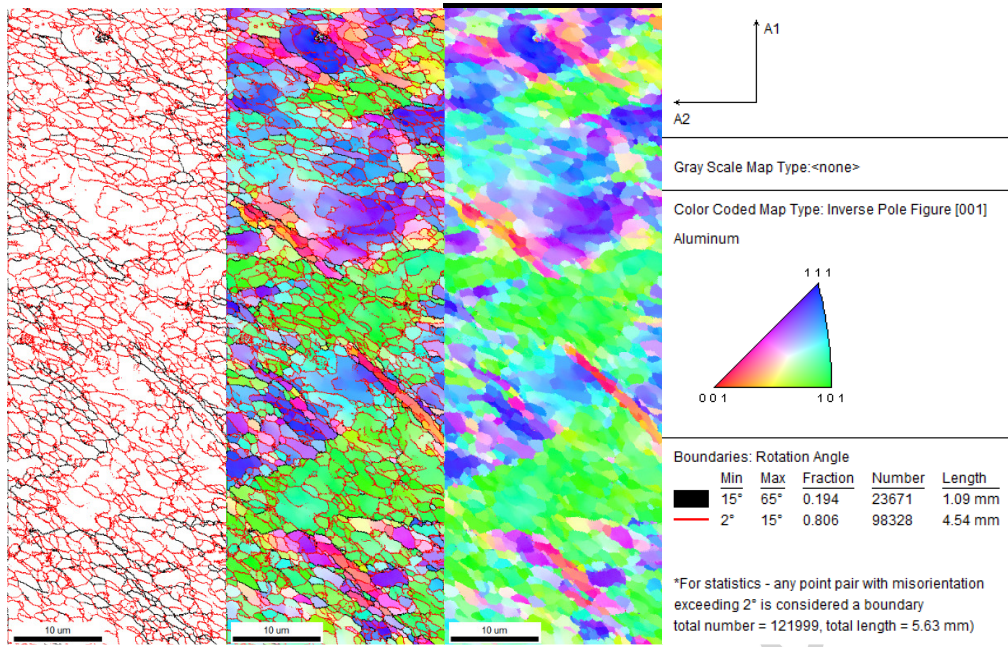
(a)

(b)

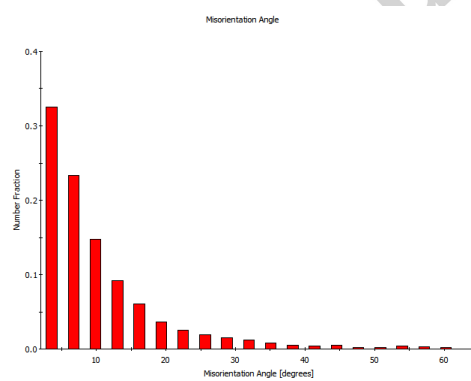
Figure 10- Microstructure of the sample in the (a) as-rolled and (b) as-annealed conditions.

Fig. 11 illustrates EBSD maps of the specimen after one pass PSE at room temperature.

The low angle grain boundaries (with misorientation angles between 2 and 15 °) are shown by the red lines and the high angle grain boundaries (with misorientation larger than 15 °) by the black lines. The results indicates the formation of cell structures at the size range of around 500 nm in both samples. However, one may notice that most cells are surrounded by low angle grain boundaries. This is quantified in Fig. 11 (b) which indicates a histogram for the misorientation angles of the microstructure. It is clear that a large fraction of grains have low angle grain boundaries. Obviously, it is expected to have more significant grain refinement, i.e., towards nano size and a larger fraction of high angle grain boundaries, by application of further PSE passes which will be discussed in future contributions of the author.



(a)



(b)

Figure 11- (a) EBSD map and (b) histogram of the distribution of misorientation angles of the microstructure after one pass PSE.

4.2.3 Hardness of processed material

The effect of PSE deformation on the hardness of the specimen is shown in Fig. 12.

Hardness is measured on the front side of the deformed sample (alongside the diagonal of the square). It is clear that hardness is increased about two times when one pass of

PSE deformation is applied to the specimen. Obviously, it is expected to have more significant strain hardening by application of further PSE passes.

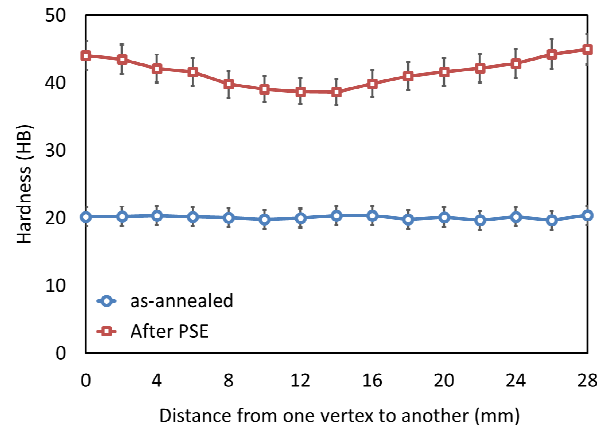


Figure 12- Variations in hardness alongside the diagonal of the specimen before and after PSE.

5 Conclusions

In this article, pure shear extrusion (PSE) is introduced as a new severe plastic deformation (SPD) technique. The theory of the method and its applications are comprehensively discussed. Strain is calculated using a geometrical approach and the die design is roughly optimized with regard to reducing frictional effects of deformation.

According to the results of this investigation, the following conclusions are made;

- 1- The feasibility of SPDing metallic samples by PSE are investigated using a die imposing a strain of 2.12. The samples are deformed for two passes with no

difficulties. Such a huge strain of 2.12 seems to be impossible to be performed using traditional SPD processes, e.g., ECAE, in one pass.

The equivalent strain increases as R increases and therefore, for acquiring very large strain in the material, using a die with large R is suggested. However, with increasing R to values larger than 3, narrow deformation zone at the sharp corners forms which makes it quite difficult for the deforming material to move against the die walls. Regarding the normalized equivalent strain over the frictional surface in the deformation zone, there is an optimum value for R equal to 2.45 at which a maximum for the ratio of normalized strain to frictional surface occurs.

- 2- The PSE process provides the possibility of severely deform metals and alloys in a combined mode of pure and simple shear. This is a unique and distinguishing capacity of the method to change the ratio of pure and simple shear without the presence of redundant work.
- 3- Verification of grain refinement and increase in hardness of the processed samples is as well an indication for efficiency of the introduced process to serve as a new SPD technique.

Appendix A:

A.1 Calculation of shear strain components (γ_{xy})

Line AB in Fig. 3 changes to $A'B'$ by PSE deformation. For calculation of the shear strains, the variations in the angles between the line AB with the x - and y -axes are considered. This angle changes from $\pi/4$ to α after the half course of PSE,

$$\gamma_{xy} = \tan\left(\frac{\pi}{4} - \alpha\right) = \sec 2\alpha - \tan 2\alpha \quad \text{Equation A - 1}$$

This may be rewritten as

$$\gamma_{xy} = \frac{1 + \tan^2 \alpha}{1 - \tan^2 \alpha} - \frac{2 \tan \alpha}{1 - \tan^2 \alpha} \quad \text{Equation A - 2}$$

since

$$\alpha = \tan^{-1} \frac{l}{L} = \tan^{-1} \frac{D^2}{L^2} \quad \text{Equation A - 3}$$

Then Eq. (A-2) becomes

$$\gamma_{xy} = \frac{1 + \left(\frac{D^4}{L^4}\right)}{1 - \left(\frac{D^4}{L^4}\right)} - \frac{2\left(\frac{D^2}{L^2}\right)}{\left(\frac{L^4 - D^4}{L^4}\right)} \quad \text{Equation A - 4}$$

By simple algebra processing

$$\gamma_{xy} = \frac{L^2 - D^2}{L^2 + D^2} \quad \text{Equation A - 5}$$

By replacing $R = \frac{L}{D}$

$$\gamma_{xy} = \frac{R^2 - 1}{R^2 + 1} \quad \text{Equation A - 6}$$

Appendix B

For calculation of frictional surface in the deformation zone, a small surface element is assumed with length dl in $x - y$ plane and dz along $z - axis$. The total frictional surface in the upper and lower deformation zone may be calculated as

$$S = 2 \left(4 \int_0^h \int_0^b dl dz \right) = 8 \int_0^{\frac{L}{2}} \int_0^{\frac{L}{2}} \sqrt{dx^2 + dy^2} dz \quad \text{Equation B - 1}$$

Where h is the height of one (upper or lower) deformation zone. since

$$\tan \theta = \frac{dy}{dx} \quad \text{Equation B - 2}$$

where θ is the instantaneous angle between one side of the deforming rhombic with x axis during deformation. θ is equal to $\pi/4$ at the onset of deformation and turns to be α as the deformation in the upper zone is finished (see Fig. 3). By replacing $\tan \theta$ in Eq. (B-2) and replacing it into Eq. (B-1), one may write

$$S = 8 \int_0^{\frac{L}{2}} \int_0^{\frac{h}{2}} \frac{dx}{\cos \theta} dz \quad \text{Equation B - 3}$$

As mentioned above, θ is changed gradually from $\pi/4$ at $z=0$ to α at $z=h$. therefore, one may write Eq. (B-4) for the relationship between θ and h

$$\theta = \frac{z}{h} \left(\alpha - \frac{\pi}{4} \right) + \frac{\pi}{4} \quad \text{Equation B - 4}$$

By replacing Eq. (B-4) in Eq. (B-3) and integration, one may obtain

$$S = \frac{4hL}{\left(\alpha - \frac{\pi}{4} \right)} \ln \left(\frac{1 + \sin(\alpha)}{(\sqrt{2} + 1) \cos(\alpha)} \right) \quad \text{Equation B - 5}$$

when $\alpha = \pi/4$ which indicates no deformation, the surface area is equal to the area of a rectangular cylinder. For the purpose of calculation of S in this case, Hopital's rule should be used and the area ends up to be

$$S = \sqrt{2}hL$$

Equation B - 6

6 References

- [1] Y. Li, J. Lu, *Materials & Design*, (2013).
- [2] M. Alizadeh, M. Samiei, *Materials & Design*, 56 (2014) 680-684.
- [3] M. Jafari, M. Enayati, M. Abbasi, F. Karimzadeh, *Materials & Design*, 31 (2010) 663-669.
- [4] A. Sharifati, S. Sharafi, *Materials & Design*, 41 (2012) 8-15.
- [5] M. Yoozbashi, S. Yazdani, T. Wang, *Materials & Design*, 32 (2011) 3248-3253.
- [6] A. Parimi, P. Robi, S. Dwivedy, *Materials & Design*, 32 (2011) 1948-1956.
- [7] M. Nili Ahmadabadi, H. Shirazi, H. Ghasemi-Nanesa, S. Hossein Nedjad, B. Poorganji, T. Furuvara, *Materials & Design*, 32 (2011) 3526-3531.
- [8] H. Zendehtdel, A. Hassani, *Materials & Design*, 37 (2012) 13-18.
- [9] S. Pasebani, M.R. Toroghinejad, *Materials Science and Engineering: A*, 527 (2010) 491-497.
- [10] V. Segal, *Materials Science and Engineering: A*, 197 (1995) 157-164.
- [11] V. Segal, *Materials Science and Engineering: A*, 271 (1999) 322-333.
- [12] I. Saunders, J. Nutting, *Metal science*, 18 (1984) 571-576.
- [13] A.P. Zhilyaev, T.G. Langdon, *Progress in Materials Science*, 53 (2008) 893-979.
- [14] P.W. Bridgman, *Studies in large plastic flow and fracture with special emphasis on the effects of hydrostatic pressure*, McGraw-Hill, 1952.
- [15] Y. Beygelzimer, D. Orlov, V. Varyukhin, *Ultrafine Grained Materials II*(as held at the 2002 TMS Annual Meeting), 2002, pp. 297-304.
- [16] Y. Saito, H. Utsunomiya, N. Tsuji, T. Sakai, *Acta materialia*, 47 (1999) 579-583.
- [17] J. Huang, Y.T. Zhu, D.J. Alexander, X. Liao, T.C. Lowe, R.J. Asaro, *Materials Science and Engineering: A*, 371 (2004) 35-39.
- [18] G. Salishchev, O. Valiakhmetov, R. Galeev, *Journal of materials science*, 28 (1993) 2898-2902.
- [19] N. Pardis, B. Talebanpour, R. Ebrahimi, S. Zomorodian, *Materials Science and Engineering: A*, 528 (2011) 7537-7540.
- [20] N. Pardis, R. Ebrahimi, *Materials Science and Engineering: A*, 527 (2009) 355-360.
- [21] N. Pardis, R. Ebrahimi, *Materials Science and Engineering: A*, 527 (2010) 6153-6156.

- [22] R.Z. Valiev, R. Islamgaliev, I. Alexandrov, Progress in materials science, 45 (2000) 103-189.
- [23] V. Segal, Materials Science and Engineering: A, 338 (2002) 331-344.
- [24] W.F. Hosford, R.M. Cadell, Metal forming mechanics and metallurgy, 1983.
- [25] A. Eivani, Materials Letters, (2014).
- [26] K. Xia, J. Wang, Metallurgical and Materials Transactions A, 32 (2001) 2639-2647.
- [27] T. Aida, K. Matsuki, Z. Horita, T.G. Langdon, Scripta materialia, 44 (2001) 575-579.
- [28] Y. Iwahashi, J. Wang, Z. Horita, M. Nemoto, T.G. Langdon, Scripta Materialia, 35 (1996) 143-146.
- [29] A. Eivani, A. Karimi Taheri, Journal of materials processing technology, 183 (2007) 148-153.
- [30] A. Eivani, A.K. Taheri, Computational Materials Science, 41 (2008) 409-419.
- [31] A. Eivani, A. Karimi Taheri, Journal of materials processing technology, 182 (2007) 555-563.
- [32] A. Eivani, S. Ahmadi, E. Emadoddin, S. Valipour, A. Karimi Taheri, Computational Materials Science, 44 (2009) 1116-1125.
- [33] A. Eivani, A. Karimi Taheri, Computational Materials Science, 42 (2008) 14-20.

Table 1- Chemical composition of the AA1050 alloy used in this study.

Element	Cu	Mg	Si	Fe	Mn	Zn	Ti	Al
Wt% Present	0.03	0.03	0.25	0.3	0.05	0.06	0.04	Balance

این مقاله، از سری مقالات ترجمه شده رایگان سایت ترجمه فا میباشد که با فرمت PDF در اختیار شما عزیزان قرار گرفته است. در صورت تمایل میتوانید با کلیک بر روی دکمه های زیر از سایر مقالات نیز استفاده نمایید:

لیست مقالات ترجمه شده ✓

لیست مقالات ترجمه شده رایگان ✓

لیست جدیدترین مقالات انگلیسی ISI ✓

سایت ترجمه فا ؛ مرجع جدیدترین مقالات ترجمه شده از نشریات معتبر خارجی